# 論文 Strain Gradient Effect on Tension Stiffening of Reinforced Concrete

**Hamed SALEM [1] and Koichi MAEKAWA [2]**

**ABSTRACT:** The aim of the present study is to discuss the strain gradient effect on tension stiffening of reinforced concrete members under flexure and/or axial loads. The analytical model is derived from the micro-bond characteristics. The local steel strain and stress are computed from which the average moment-curvature relationship is derived. The average crack spacing is simply computed by a stress-based cracking criterion. A comparison with experimental observations was carried out to verify the effectiveness of analysis. The analysis fairly agrees with the experimental results.
**KEY WORDS:** bond-slip-strain, tension stiffening, crack spacing, strain gradient, flexure.

## 1. INTRODUCTION

It has been widely known that crack spacing in reinforced concrete members subjected to axial tension is different from those members under bending moments (CEB-FIP [1]). Since the crack spacing is an important factor that affects the stiffening behavior of cracked concrete (Salem and Maekawa, [7], [8]), it is considered that the strain gradient across the cross section of RC members plays a significant role on the tension stiffening. In this study, this role is studied. Crack spacing is predicted by a simple stress-based criterion (Salem and Maekawa, [7], [8]). In this method, the local stress of concrete is checked and cracking is introduced whenever the local stress reaches the cracking strength of concrete.

**Fig. 1** illustrates a schematic drawing to explain the role of strain gradient on members cracking. In this figure, two members are shown, one is under axial tension while the other is under pure flexure. It was assumed that the height of the tension member is half that of the flexure member. In other words, the concrete portion that resists tensile stresses, at the middle non-cracked section of the flexure member, has the same area as that of the tension member. However, since the concrete stresses at the middle section of the flexure member is linearly distributed in consistence with the linear strain distribution at that section, the maximum stress will be double that of the tension member under the same loading level. As a result, more cracks are most likely to talk place in the flexure members.

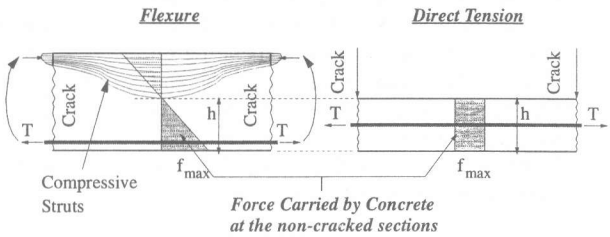


Fig. 1 Cracking Response in Axial Tension and Flexure Members

## 2. MODELING ASSUMPTIONS

(1) There is no real physical slip between concrete and reinforcement at the location of reinforcement (Okamura and Maekawa, [4]). In other words, the crack width at the steel location is zero and the concrete has the same elongation of reinforcement at that location. Following this fact, the bond-slip-strain model of Shima et al [3] is used.

[1] Department of Civil Engineering, The University of Tokyo, Ph. D, Member of JCI
[2] Department of Civil Engineering, The University of Tokyo, Dr. Eng., Member of JCI

(2) Strain distribution along the non-cracked section is linear following Bernoulli's assumption. This implies that the assumption is restricted to the shallow members, as it is not realistic for deep beams or shear walls.
(3) The bond properties between steel and concrete in flexure members are the same as tension members. Due to strain gradient, there might be some difference but not significant. However, this is out of target of the present study.
(4) Cracking of concrete takes place whenever the local concrete stress reaches the tensile strength. In this model, the average crack spacing (Salem and Maekawa, [7], [8]) is applied.
(5) The location of the neutral axis is linearly changing between the crack location and the middle non-cracked section (see **Fig. 2**). In this region concrete is still non-cracked but the tensile resistance is not fully utilized due to its dependence on the amount of stress transferred by bond with the steel bar.
(6) For large-scale members the concept of effective RC zones developed by An et al [9] is adopted. In this case, only the RC zone is considered to resist the tensile load and is responsible for cracking if its resistance is lower than the tensile load as illustrated in **Fig. 3**.
(7) For the concrete under compression, the elasto-plastic and fracture model developed by Maekawa and Okamura [2] is adopted.

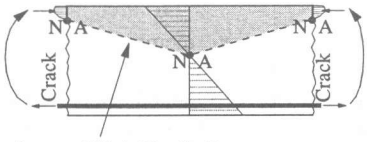


Fig. **2** Assumed Neutral Axis Distribution between Cracked and Non-cracked Sections

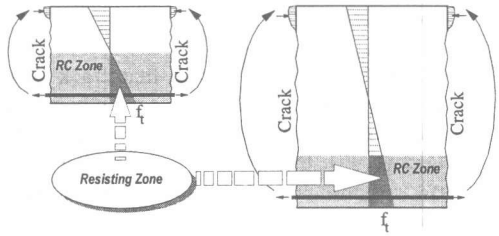


Fig. **3** Effective Reinforced Concrete Zone Concept

## 3. ANALYSIS

### 3.1 COUPLED FLEXURE AND AXIAL LOADS

In case of flexure coupled with axial loads, the neutral axis at the non-cracked section is shifted up or down depending on the types of axial load, tension and compression. The shifted distance is determined from the ratio of the axial load to the bending moment. From **Fig. 4**, it can be shown that the shifted distance is,

$$x = \left(\frac{N}{M}\right)\left(\frac{h^2}{12}\right) \qquad (1)$$

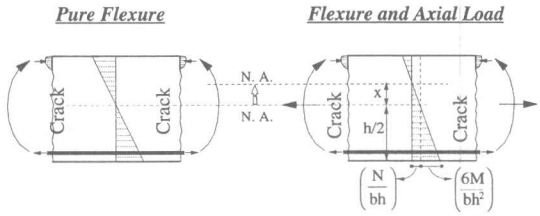


Fig. **4** Neutral Axis Shift for Coupled Axial and Flexure Loading

where, N is the axial load, M is the bending moment and h is the height of the cross section.

### 3.2 COMPUTATIONS SCHEME

The analytical scheme is similar to the analysis under axial tension by Salem and Maekawa [7], [8]. Analysis scheme is shown in **Fig. 5**. In the scheme, the local bond stresses along steel bar are computed by solving the nonlinear governing bond equations satisfying both the slip compatibility and the boundary conditions of zero slip and zero bond stresses at the midway between two adjacent cracks. The bond-slip-strain model developed by Shima et al [3] is adopted. Deterioration of bond stresses that occurs due to crushing and spalling of concrete close to crack surface are taken into account by the implementation of the bond deterioration model of Qureshi and Maekawa [6].

Calculating the local bond stresses, local stresses and strains of steel and concrete are computed. Cracking of concrete is introduced whenever the local concrete stress reaches the cracking strength. The crack spacing used in analysis is the average crack spacing.

Sectional bending moments and axial forces are computed by integrating the internal stresses at crack location. At cracked section, the neutral axis location is decided by iterative procedure so that the equilibrium among internal forces and external forces is maintained. The curvature concerned here is the average curvature including cracked concrete and non-cracked concrete. This curvature is computed from Bernoulli's assumption as,

$$\Phi = \frac{\bar{\varepsilon}}{\bar{y}} \qquad (2)$$

where, $\bar{\varepsilon}$ is the average axial strain along the reinforcing bar and $\bar{y}$ is the average distance between the neutral axis and the steel bar, which can be computed by adopting assumption No. (5). Thus, the moment-average curvature relationship can be computed.

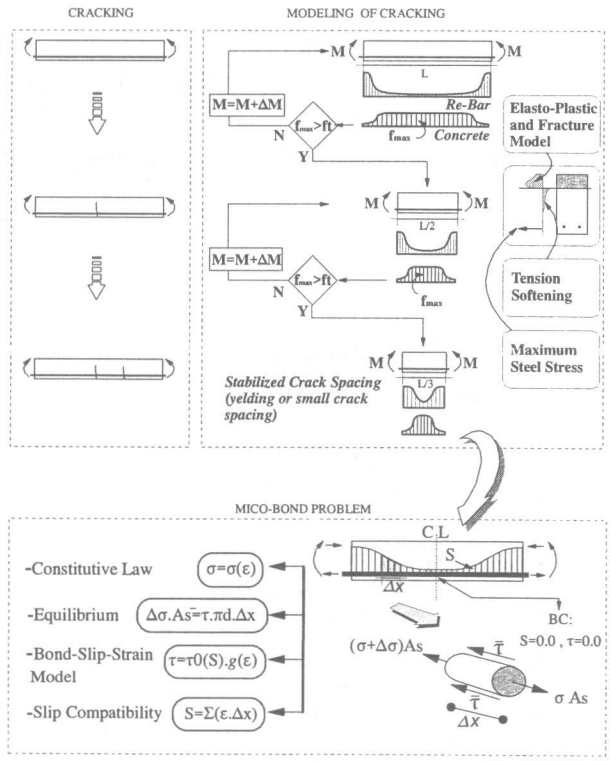


Fig. 5 Analysis Scheme

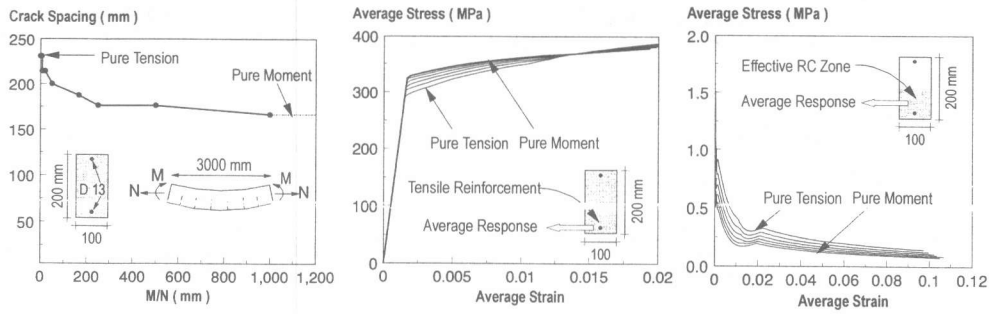


(a) (b) (c)

Fig. 6 Strain Gradient Effect on Tensile Response of RC

The effect of strain gradient is discussed by comparing the response of RC members subject to different combinations of normal and bending moments as shown in **Fig.6**. In **Fig. 6(a)** the computed average crack spacing is shown as a function of the ratio of bending moment to normal force. As expected the crack spacing gets smaller by increasing the ratio of M/N and it is the smallest for pure moment. As a result, the average stress of reinforcement is increasing while the average response of concrete is decreasing when the ratio of M/N increases due to the reduction in the crack spacing (see **Fig. 6(b)** and **(c)**).

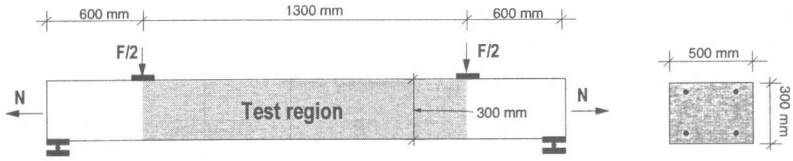


Fig. 7 Load Set-Up and Specimens tested under coupled axial loads and flexure ( Polak and Killen [11])

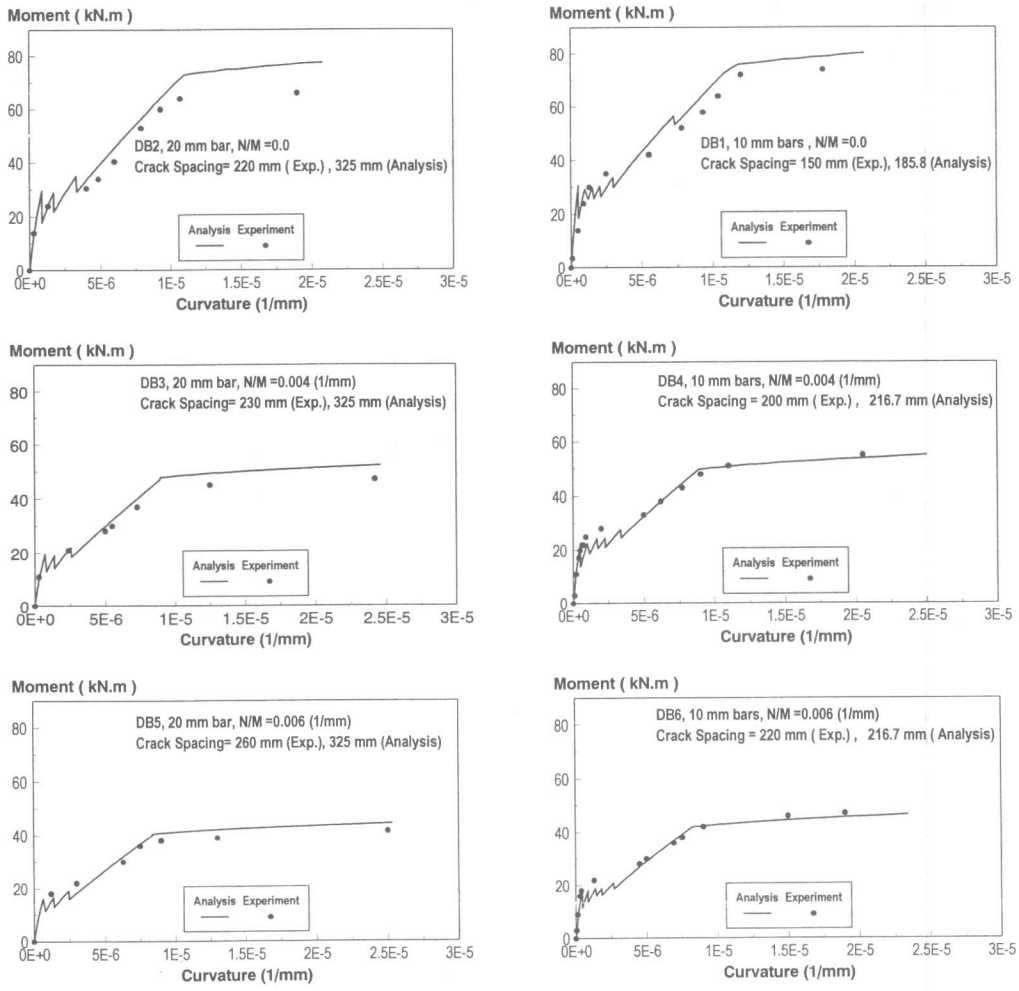


Fig. 8 Experimental Verifications (A Comparison with The Experiments of Polak and Killen [11])

## 4. EXPERIMANTAL VERIFICATION

For verification of the proposed model, comparison with the experimental findings by both Polak and Killen [11] and Ruiz et al [10] is conducted. The experiments by Polak and Killen were designated to normal reinforced concrete while those by Ruiz et al. were of lightly reinforced concrete.

### 4.1 NORMALLY REINFORCED CONCRETE BEAMS

Specimens of Polak and Killen [11] were 500 mm in width and 300 mm in height and having a reinforcement ratio of 0.4 %. Three of the specimens (DB2, DB3, DB5) were reinforced with 20 mm reinforcing bars and three (DB1, DB2, DB6) were with 10 mm bars. Specimens DB1 and DB2 were tested in pure bending, DB3 and DB4 in tension and bending with the ratio of N/M=0.004 (1/mm), and DB5 and DB6 in tension and bending with the ratio of N/M=0.006 (1/mm). Specimens' details are shown in **Fig. 7** and experimental results and analysis are shown in **Fig. 8**. Fairly good agreement with the experimental results can be observed in the figures.

### 4.2 LIGHTLY REINFORCED CONCRETE BEAMS

Specimens of Ruiz et al. [10] were lightly micro-reinforced concrete beams specimens with reinforcement ratios ranging from 0.065% up to 0.26 %. Beams depth varies from 75 mm up to 300 mm and reinforcement is 2.5 mm ribbed wires with proof stress of 568 MPa. Loading set-up and specimen details are shown in **Fig. 9**. The specimens were tested in a three point bending as shown in **Fig. 9**. In the experiments, due to the low reinforcement, all the beams had a single localized crack in the middle of the specimens. In the analysis of these specimens, the beam central deflection due to rotation at the middle section was computed by a simple triangular similarity as shown in **Fig. 10**. This deflection is equal to,

$$\delta = \left(\frac{L}{2}\right)\left(\frac{S}{h-C}\right) \tag{3}$$

where, L is the beam length, S is the steel slip at the crack location and C is the concrete cover.

A comparison of the experimental results with the analytical ones is shown in **Fig. 11**, which shows a reasonable agreement.

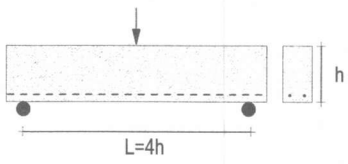


Fig. **9** Load Set-Up of Test Beams by Ruiz et al [10]

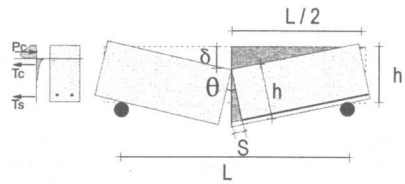


Fig. **10** Centeral Deflection due to Central Rotation in Test Beams of Ruiz et al [10]

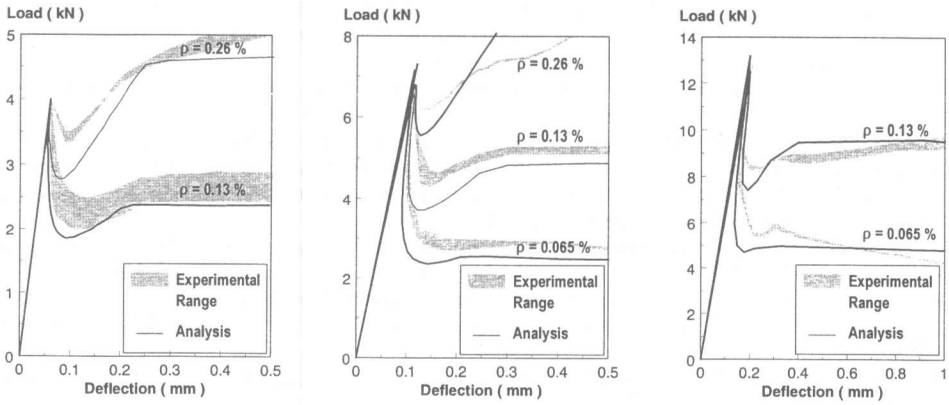


Fig. **11** Experimental Verifications (A Comparison with The Experiments of Ruiz et al [10])

### 4.3 CRACK SPACING PREDICTION

For checking the prediction of crack spacing, the calculated crack spacing is compared with the observed one for different experiments carried by Polak [11], [12], Hauke [13] as shown in **Fig. 12**. The test specimens are subjected to uniform bending moments coupled with axial loads. The same comparison is carried out for the CEB-FIP code as shown in the figure. From these comparisons, fairly good agreement can be observed between the proposed model and the experiments.

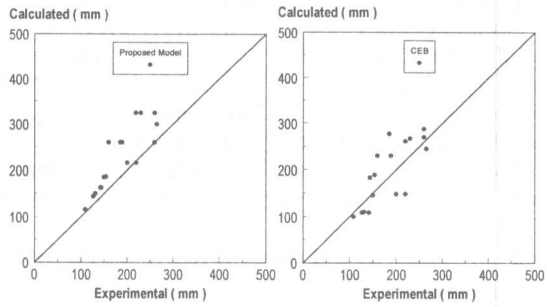


Fig. **12** Comparison of the Model and Experimental Crack Spacing

## 5. CONCLUSIONS

1) Based on the micro-bond characteristics, response of reinforced concrete beams under flexure and/or axial tension is computed. The analysis can cover cases of both normally and lightly reinforced concrete beams.
2) Crack spacing of flexure members is generally smaller than that of axial tension members. As a result, the average response of steel in flexure members gets higher than that of axial tension members. On the other hand, the average response of concrete in flexure members gets smaller than that of axial tension members.

## REFERENCES


1. CEB: CEB-FIP model code, 1978.
2. Maekawa, K. and Okamura, H.: The Deformational Behavior and Constitutive Equation of Concrete Using the Elasto-Plastic and Fracture Model, Journal of the Faculty of Engineering, The University of Tokyo (B), Vol. 37, No. 2, pp. 253-328, 1983.
3. Shima, H., Chou, L. and Okamura, H.: Micro and Macro Models for Bond in Reinforced Concrete" Journal of The Faculty of Engineering, The University of Tokyo (B), Vol. 39, No 2, 1987.
4. Okamura, H. and Maekawa, K.: Nonlinear Analysis and Constitutive Models of Reinforced Concrete, Gihodo, Tokyo, 1991.
5. Uchida, Y., Rokugo, K. and Koyanagi, W.: Determination of Tension Softening Diagrams of Concrete by Means of Bending Tests, Proc. of JSCE, Vol. 14, No. 426, 1991.
6. Qureshi, J. and Maekawa, K.: Computational Model For Steel Bar Embedded in Concrete Under Combined Axial Pullout and Transverse Shear Displacement, Proc. of JCI, Vol.15, No. 2, pp 1249-1254, 1993.
7. Salem, H. M. and Maekawa, K.: Tension Stiffness for Cracked Reinforced Concrete Derived from Micro-bond Characteristics, Proc. of JCI, Vol.19, No. 2, pp 549-554, 1997.
8. Salem, H. M. and Maekawa, K.: Coupled Bond and Bridging Stress Transfer in Cracked Reinforced Concrete, Proc. of FRAMCOS-3, Gifu, Japan, Vol.2, pp 1353-1362, 1998.
9. An, X., Maekawa, K. and Okamura, H.: Numerical Simulation of Size Effect in Shear Strength of RC Beams, Journal of Materials, Concrete Structures, Pavements, JSCE, Vol. 35, No. 564, pp. 297-316, 1997.
10. Ruiz, G., Elices, M. and Planas, J.: Experimental Study of Fracture of Lightly Reinforced Concrete Beams, Materials and Structures, Vol. 31, pp. 683-691, 1998
11. Polak, M. and Killen, D.: The Influence of The Reinforcing Bar Diameter on The Behavior of Members in Bending and In-Plane Tension, ACI Structural Journal, Vol. 95, No. 5, pp. 471-479, September, 1998.
12. Polak, M. and Blackwell, K.: Modeling Tension in Reinforced Concrete Members Subjected to Bending and Axial Loads, Journal of Structural Engineering, ASCE, Vol. 124, No. 9, pp. 1018-1024, September, 1998.
13. Hauke, B.: Three-Dimensional Modeling and Analysis of Reinforced Concrete and Concrete Composites, Ph. D. Thesis, The University of Tokyo, 1998.